Materials Science & Engineering C 82 (2018) 121–129

Contents lists available at ScienceDirect

Materials Science & Engineering C

journal homepage: www.elsevier.com/locate/msec

Fabrication and preliminary study of a biomimetic tri-layer tubular graft based on fibers and fiber yarns for vascular tissue engineering

Tong Wu[a,1], Jialing Zhang[b,1], Yuanfei Wang[c], Dandan Li[d], Binbin Sun[a], Hany El-Hamshary[e,f], Meng Yin[b,*], Xiumei Mo[a,**]

[a] State Key Lab for Modification of Chemical Fibers and Polymer Materials, College of Chemistry, Chemical Engineering and Biotechnology, Donghua University, Shanghai 201620, China
[b] Department of Cardiothoracic Surgery, Shanghai Children's Medical Center, Shanghai Jiaotong University School of Medicine, Shanghai 200127, China
[c] State Key Laboratory of Bioreactor Engineering, School of Resources and Environmental Engineering, East China University of Science and Technology, Shanghai 200237, China
[d] College of Material Science and Engineering, Donghua University, Shanghai 201620, China
[e] Department of Chemistry, College of Science, King Saud University, Riyadh 11451, Saudi Arabia
[f] Department of Chemistry, Faculty of Science, Tanta University, Tanta 31527, Egypt

ARTICLE INFO

Keywords:
Tri-layer tubular graft
Fibers
Fiber yarns
Vascular tissue engineering

ABSTRACT

Designing a biomimetic and functional tissue-engineered vascular graft has been urgently needed for repairing and regenerating defected vascular tissues. Utilizing a multi-layered vascular scaffold is commonly considered an effective way, because multi-layered scaffolds can easily simulate the structure and function of natural blood vessels. Herein, we developed a novel tri-layer tubular graft consisted of Poly(L-lactide-*co*-caprolactone)/collagen (PLCL/COL) fibers and Poly(lactide-*co*-glycolide)/silk fibroin (PLGA/SF) yarns *via* a three-step electrospinning method. The tri-layer vascular graft consisted of PLCL/COL aligned fibers in inner layer, PLGA/SF yarns in middle layer, and PLCL/COL random fibers in outer layer. Each layer possessed tensile mechanical strength and elongation, and the entire tubular structure provided tensile and compressive supports. Furthermore, the human umbilical vein endothelial cells (HUVECs) and smooth muscle cells (SMCs) proliferated well on the materials. Fluorescence staining images demonstrated that the axially aligned PLCL/COL fibers prearranged endothelium morphology in lumen and the circumferential oriented PLGA/SF yarns regulated SMCs organization along the single yarns. The outside PLCL/COL random fibers performed as the fixed layer to hold the entire tubular structure. The *in vivo* results showed that the tri-layer vascular graft supported cell infiltration, scaffold biodegradation and abundant collagen production after subcutaneous implantation for 10 weeks, revealing the optimal biocompatibility and tissue regenerative capability of the tri-layer graft. Therefore, the specially designed tri-layer vascular graft will be beneficial to vascular reconstruction.

1. Introduction

Cardiovascular diseases are considered to be the leading cause of death globally [1,2]. Although the native vein and artery sections remain the best way to repair defected blood vessels *via* peripheral or coronary bypass procedures, their availability is still limited when the autologous blood vessels are occluded or diseased, or the size is not matched with the defected site [3]. Hence, it is urgently needed to develop clinically approved vascular prostheses as alternatives due to the morbidity and mortality caused by vascular diseases and disorders. Nowadays, some commercial artificial blood vessels such as Dacron or e-PTFE grafts have been commonly used for vascular repair [3]. However, the artificial grafts occurred failure for long-term patency and especially for the small-diameter vascular application, because the small-diameter vascular graft increased the danger of thrombosis and occlusion [4]. In the recent years, tissue-engineered scaffolds based on nanofibers have been developed and employed in different biomedical applications [5–12]. Based on the strategies of tissue engineering, large amounts of tissue-engineered vascular scaffolds with good biocompatibility, controllable mechanical properties, and manageable biodegradability have been designed [13–18]. Tissue-engineered vascular grafts can be easily manufactured because of the stability and

* Corresponding author at: Department of Cardiothoracic Surgery, Shanghai Children's Medical Center, Shanghai Jiaotong University School of Medicine, Shanghai 200127, China.
** Corresponding author at: College of Chemistry, Chemical Engineering and Biotechnology, Donghua University, 2999 North Renmin Road, Shanghai 201620, China.
E-mail addresses: yinmengmdphd@163.com (M. Yin), xmm@dhu.edu.cn (X. Mo).
[1] Author Contributions: Tong Wu and Jialing Zhang contributed equally to this work.

http://dx.doi.org/10.1016/j.msec.2017.08.072
Received 18 June 2017; Received in revised form 13 August 2017; Accepted 16 August 2017
Available online 17 August 2017
0928-4931/

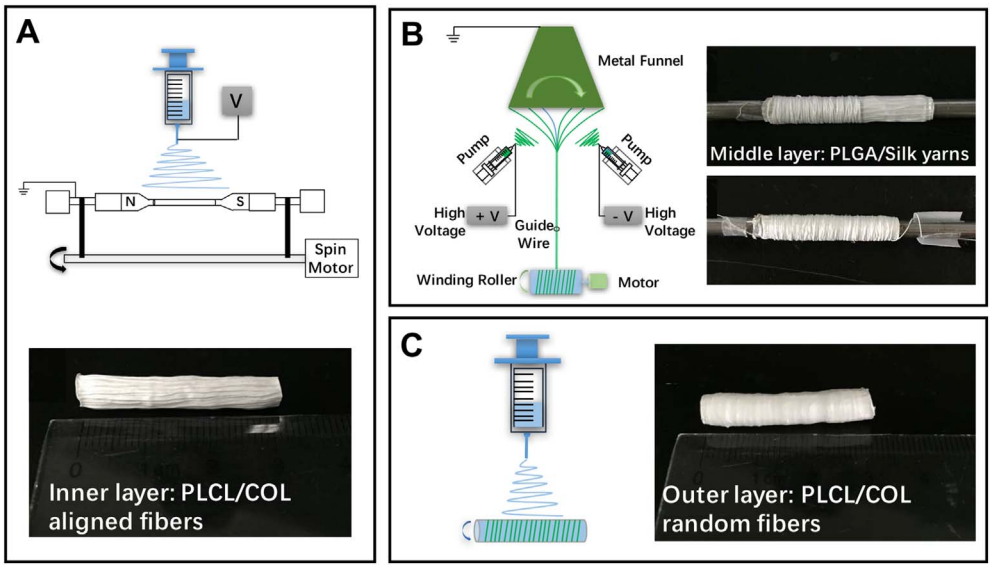

Fig. 1. The schematic diagram showing the fabrication of tri-layer tubular graft: (A) Fabrication of PLCL/COL axially aligned fibers (inner layer) *via* the general electrospinning method with a customized rotating collector; (B) Fabrication of the PLGA/SF yarns by a customized electrospinning equipment. The PLGA/SF yarns served as the middle layer by twining on the inner layer in circumferential orientation; (C) Fabrication of a thin layer of PLCL/COL random fibers (outer layer) on the prepared complex (inner and middle layers) to fix the whole layers.

maneuverability of the preparation technologies such as electrospinning, phase separation, freeze drying, and three-dimensional printing, *etc.* [19–22].

To biomimetic the structure and function of native blood vessels, designing multi-layered vascular scaffolds is an effective way. Electrospinning has been widely used, because it is easier to blend or mix various materials and build non-delamination layers to develop multi-layered scaffolds [23–30]. McClure et al. fabricated a three-layered electrospun matrix to mimic native arterial architecture using polycaprolactone, elastin, and collagen [27]. The results indicated that the graft had sufficient tensile strength, dynamic compliance, suture retention, and burst strength by altering layer properties. Then, they further developed a tri-layered vascular graft composed of polycaprolactone, elastin, collagen, and silk [28]. The results revealed the optimization of graft properties and concluded that the multi-layered graft architecturally mimicked the native vascular wall and mechanically matched the gold standard of vessel replacement, saphenous vein [28]. Zhang and Han et al. designed multi-layered small-diameter vascular scaffolds which had dual-loading of vascular endothelial growth factor (VEGF) and platelet derived growth factor (PDGF) [23,24]. The grafts synergistically regulated the growth of vascular endothelia cells in lumen and smooth muscle cells on the exterior through the controlling of VEGF/PDGF releasing. Valence et al. compared two bilayered vascular grafts with different porosity and evaluated their potential for surgical applicability and tissue regeneration [25]. The results demonstrated that the graft with a low-porosity layer on the lumen and a high-porosity layer on the adventitial side reduced blood leakage, promoted cell invasion from the surroundings, and did not affect the endothelialization rate. Therefore, it is of foremost importance to design a multi-layered microarchitecture for biodegradable vascular prostheses.

The endothelium in the native blood vessel is a simple but well-organized monolayer, and the orientation of endothelia cells can regulate biological signaling events including intracellular protein expression, cytoskeleton construction, and cell-to-cell interactions [31–34]. Correspondingly, the smooth muscle cells are spindle-shaped and aligned their long axis perpendicular to the blood vessel length, which plays an important role in maintaining elasticity, mechanical strength, and vasoactive responsiveness of blood vessels [35–38]. To simulate the tri-layer structure of the native blood vessel and the function of vascular lumen and media, a novel tri-layered vascular graft was designed and fabricated through a three-step electrospinning method in this study. The graft consisted of axially aligned Poly(L-lactide-*co*-caprolactone)/collagen (PLCL/COL) fibers in lumen, circumferentially oriented Poly(lactide-*co*-glycolide)/silk fibroin (PLGA/SF) yarns in media, and random PLCL/COL fibers in adventitia. Then, the mechanical properties, endothelia cells and smooth muscle cells proliferation and morphology, and *in vivo* evaluation of subcutaneous implantation in mice were assessed to determine the potential application of the tri-layer vascular graft for vascular tissue engineering.

2. Materials and methods

2.1. Materials

Poly(L-lactide-*co*-caprolactone) (PLCL, LA:CL = 50:50; Mn: 450,000) was purchased from Jinan Daigang Biomaterial Co., Ltd. (Jinan, China). Porcine-derived type I collagen (Mn: 100,000) was supplied by ChengDu Kele Bio-tech Co., Ltd. (Chengdu, China). 1,1,1,3,3,3-hexafluoro-2-propanol (HFIP) was acquired from Shanghai Fine Chemicals Co., Ltd. (Shanghai, China). Poly(lactide-*co*-glycolide) (PLGA, LA:GA = 82:18; IV(dl/g): 1.9) was supplied by Jinan Daigang Biomaterial Co., Ltd. (Jinan, China). *Bombyx mori* silkworm cocoons were supplied by Jiaxing Silk Co. Ltd. (China) and the regenerated silk fibroin (SF) was prepared as previously reported [39]. Glutaraldehyde aqueous solutions (GA, 25%) were acquired from Sinopharm Chemical Reagent Co., Ltd. (Shanghai, China). Human Umbilical Vein Endothelial Cells (HUVECs) and smooth muscle cells (SMCs) were obtained from the Institute of Biochemistry and Cell Biology (Chinese Academy of Sciences, China). All the cell culture reagents were provided by Gibco Life Technologies Co., (USA) unless specified.

2.2. Fabrication

PLCL/collagen (PLCL/COL) blends were dissolved in HFIP with a weight ratio of 3:1 and at a concentration of 10%. PLGA/Silk (PLGA/SF) composites were dissolved in HFIP with a weight ratio of 3:1 and at a concentration of 15%. The tri-layer tubular graft was fabricated *via* three steps. Firstly, the axially aligned PLCL/COL fibers in inner layer were fabricated by placing a collector in a magnetic field generated from N-poles to S-poles (Fig. 1A). A custom-made Teflon conduit mold served as the collector (the diameter was 4 mm, the length was 3 cm, and the rotating speed was 50 rpm). A high voltage of 12 kV, a flow rate of 1.0 mL/h, and a collect distance of 12 cm were applied, and the axially aligned PLCL/COL fibers were collected because of the axial magnetic environment in the electrospinning process. The PLGA/SF yarns were pre-prepared *via* an electrospinning equipment with double-nozzle system (TFS-700, Beijing Technova Technology Co., Ltd., China)

as presented in Fig. 1B. The rotatable funnel with a rotating rate of 450 rpm was utilized to twist fibers to yarns. A rotatable rod with a low rotating speed at 7 rpm and horizontal movement of 10 mm/min was used to collect yarns. Two spinnerets in the opposite directions were severally applied with the positive high voltage at + 9 kV and the relative negative high voltage at − 9 kV, and conducted with the flow rates at 0.02 mL/min and 0.032 mL/min, respectively. Then, the pre-prepared PLGA/SF yarns were served as the middle layer in the graft by twining on the inner layer in circumferential orientation. The double ends of yarns were fixed on the collector by the adhesive tape (Fig. 1B). Finally, the inner and middle layer was performed as the collector with a rotating rate at 200 rpm to gather the random PLCL/COL fibers (Fig. 1C). The random PLCL/COL fibers in the outer layer served as the adhesive to fix the whole layers of the tubular graft. The obtained tri-layer tubular graft was crosslinked by GA vapor for 15 min and stored in the vacuum oven before further evaluation.

2.3. Characterization

The structure and morphology of the tri-layer tubular graft was observed by a digital camera and a scanning electron microscope (SEM) (Phenom XL, Phenom-World B.V., Netherlands). A Fourier transform infrared spectroscopy (FTIR) (Thermo Electro AVATAR 380, USA) was utilized to test the characteristic functional groups of PLCL/COL fibers and PLGA/SF yarns. The tensile mechanical properties of PLCL/COL fibers (50 mm × 10 mm, n = 3) and one single PLGA/SF yarn (50 mm length, n = 3) were measured by a universal material testing machine (H5K-S, Hounsfield, UK). The tensile and compressive mechanical properties of the tri-layer tubular graft (4 mm inner diameter and 10 mm length, n = 3) were tested by a tensile and compression testing machine (HY-940FS, Hengyu Instrument Co., Ltd., China). The compressive tests were performed with 10 cycles when elastic deformation was 50%. The curves were obtained using the Scidavis software.

2.4. HUVECs proliferation on PLCL/COL fibers

HUVECs were incubated in Dulbecco's modified Eagle's medium (DMEM) medium with 10% fetal bovine serum and 1% antibiotic–antimycotic at an atmosphere of 37 °C, 5% CO_2 and 95% humidity. The culturing medium was refreshed every two days. The aligned and random PLCL/COL fibrous mats were punched into several slides with 14 mm diameter, placed in the 24-well plates, and secured with the stainless rings. The tissue culture plates (TCP) were used for the control. Before seeding HUVECs, the samples were disinfected under 75% ethanol vapor overnight and followed by rinsing with sterilized PBS solution. Then, the samples were soaked in the DMEM medium and placed in the incubator for 2 h. The HUVECs were seeded on the PLCL/COL random fibers, PLCL/COL aligned fibers and TCP with a density of 1×10^5 cells/mL. The culturing medium was changed every other day.

HUVECs proliferation on the different samples were evaluated by a cell counting kit-8 (CCK-8, Dojindo Lab., Japan) after culturing cells for 1, 3 and 6 days. At each time point, the medium was removed and the fresh medium with 10% CCK-8 was added. After incubating for 2 h at 37 °C, the aliquots were extracted into a 96-well plate, and the absorbance was measured at 450 nm by an Enzyme-labeled Instrument (Multiskan MK3, Thermo, USA) (n = 6). When HUVECs were cultured for 3 days, the samples were washed with PBS solution and fixed with 4% paraformaldehyde. Then, 0.1% Triton X-100 (Sigma, USA) was used to permeabilize samples for 5 min, and 2% bull serum albumin (BSA) solution was used for blocking. After each process, the samples were rinsed with PBS for three times. The rhodamine-conjugated phalloidin (Invitrogen, USA) was used to stain the cytoskeletons of cells. The samples were observed under the inverted fluorescence microscope (IFM, Olympus IX71, Japan).

2.5. SMCs proliferation on PLGA/SF yarns

SMCs were incubated in the same conditions with HUVECs as above mentioned. The PLGA/SF fibers were punched into the slides, and the PLGA/SF yarns were wrapped on the 14 mm-diameter cover slips with TCP as the control group as well. The samples were sterilized by 75% ethanol vapor and pre-processed with DMEM medium. Then, SMCs were seeded on the samples with a density of 1×10^5 cells/mL and cultured for 6 days. SMCs proliferation was measured using the CCK-8, and SMCs morphologies on different samples were evaluated by fluorescence staining with rhodamine-conjugated phalloidin.

2.6. Subcutaneous implantation in mice

All experimental procedures relating to animals were performed under institutional guidelines for animal care and approved by the Animal Ethics Committee of Shanghai Children's Medical Center, Shanghai Jiaotong University School of Medicine (Shanghai, China). Ten male nude mice (7 weeks old) were purchased from Shanghai Slaccas Experimental Animal Ltd. (Shanghai, China) and used for subcutaneous implantation in 10 weeks. Before *in vivo* implantation, the grafts were processed with ethylene oxide for sterilization. Then, 400 mg/kg of chloral hydrate was intraperitoneally injected in animals for anesthetization. The implantation sites on the back of mice were sterilized by iodine solution, and two subcutaneous pockets were produced on each side of dorsa. The graft with 4 mm in inner diameter and 10 mm in length was implanted into each pocket, and the cuts were sutured.

2.7. Histological analysis

After gross examination, the grafts were harvested and used for histological analysis. The collected samples were fixed in 4% paraformaldehyde, embedded in paraffin and sectioned. Then, the sections were stained with hematoxylin and eosin (H & E) and Masson's trichrome for assessment.

2.8. Statistics analysis

Statistics analysis was completed using origin 9.0 (Origin Lab Inc., USA). All the values were averaged at least in triplicate and presented as means ± standard deviation (SD). Statistical differences were determined by the analysis of one-way ANOVA and differences were considered statistically significant at $P < 0.05$ level.

3. Results and discussion

3.1. Morphology and structure of the tri-layer tubular graft

The tri-layer tubular graft was fabricated *via* the three-step electropsinning method as displayed in Fig. 1A–C. The rotating collector with N-poles and S-poles formed the axial magnetic field environment during the electrospinning process, and therefore contributed to producing the axially aligned PLCL/COL fibers in the inner layer (Fig. 1A). The PLGA/SF yarns in the middle layer were prepared by the doube-nozzle electrospinning system (Fig. 1B). The PLGA/SF yarns can be arranged in circumferential orientation by precisely twining on the inner layer. The outermost thin layer of PLCL/COL random fibers was generated by the simple single-nozzle electrospinning, and the random fibers fixed the entire layers of the tubular graft (Fig. 1C).

The SEM images in Fig. 2 demonstrate the structure and morphology of the tri-layer tubular graft. Fig. 2A shows the cross section of three layers, where the inner/outer surfaces were dense fibers and the middle layer consisted of loose yarns. The PLCL/COL aligned fibers (Fig. 2B) and PLCL/COL random fibers (Fig. 2D) had the diameter of 336.90 ± 107.27 nm and 361.15 ± 136.91 nm, respectively

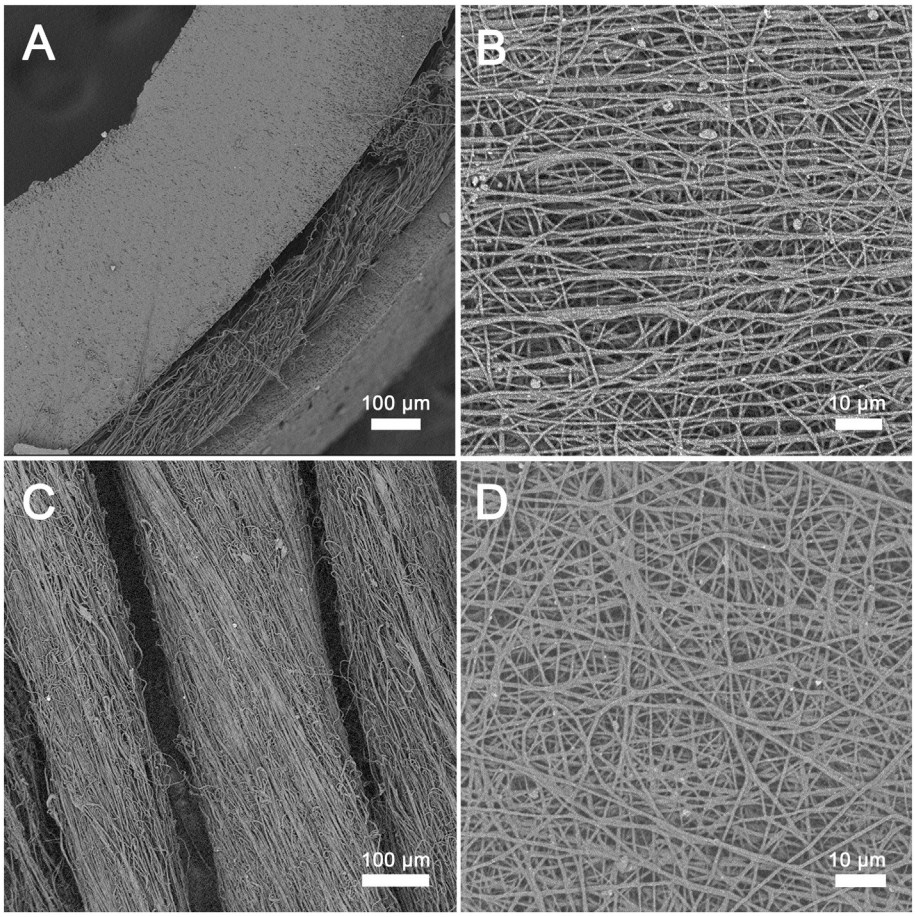

Fig. 2. SEM images showing the morphology of (A) the cross section of the tri-layer tubular graft, (B) the aligned PLCL/COL fibers in the inner layer, (C) the PLGA/SF yarns in the middle layer, and (D) the random PLCL/COL fibers in the outer layer.

(Table 1). In comparison, the PLGA/SF yarns arranged in orientation (Fig. 2C) and possessed the diameter of 206.17 ± 46.23 μm (Table 1), and the gap between the adjacent yarn was 39.02 ± 6.25 μm. The PLCL/COL fibers presented an alignment in the axial direction (Fig. 1A and Fig. 2B), and the PLGA/SF yarns had the circumferential orientation (Fig. 1B and Fig. 2C). The external surface of PLCL/COL random fibers presented the random fiber distribution (Fig. 1C and Fig. 2D). By regulating the electrospinning time, the thickness of each layer can be varied. In this study, we fabricated the tri-layered graft with thick inner layer to support the tubular structure and avoid blood leakage. Tiny amounts of random fibers in the outer layer were enough to fix the yarns on the inner layer.

We used different polymer/protein fibers for different layers mainly due to the operability during electrospinning and the distinctive biodegradability of varied materials. In our previous study, PLCL/COL fibers supported the macrostructure for almost 4 months *in vitro* [40]. *In vivo* studies also demonstrated that PLCL/COL based scaffolds could support tissue regeneration for > 8 weeks [41,42]. Hence, the PLCL/COL fibers were used as the inner and outer layer for holding the tubular structure. By contrast, the middle layer was designed to be porous and fast-biodegraded to support more and more cells' infiltration during *in vivo* implantation. PLGA is one of the top biodegradable synthetic polymers used for tissue engineering due to the ease of controlling its mechanical properties and biodegradation rate [43]. Besides, in our trial for fabricating fiber yarns, PLGA/SF presented the advantages to obtain homogeneous and continuous yarns. Hence, PLGA/SF was used for the middle layer of the vascular scaffold.

3.2. FTIR results

Fig. 3 demonstrates the FTIR results of PLCL/COL fibers and PLGA/SF yarns. The absorption peaks at 1652 cm^{-1} (amide I) and 1540 cm^{-1} (amide II) in all samples represented the existence of protein (collagen or silk fibroin) [42,44,45]. The strong bonds at 1757 cm^{-1} were observed due to the presence of the carbonyl group (C═O stretch) in PLCL and PLGA [44,46]. Additionally, the bonds at 1184 cm^{-1} were attributed to the symmetric and asymmetric vibrations of C−O in esters, thus also highlighted the existence of PLGA and PLCL [46].

3.3. Mechanical properties

Fig. 4A-C demonstrates the tensile mechanical properties of PLCL/COL fibers and PLGA/SF yarns. The PLCL/COL aligned fibers in the inner layer had an ultimate stress of 23.03 ± 2.00 MPa and a largest

Table 1
Diameter, tensile stress and elongation of PLCL/COL fibers and PLGA/SF yarns.

	Fiber/Yarn diameter	Tensile stress (MPa)	Tensile elongation (%)
PLCL/COL aligned fibers (parallel)	336.90 ± 107.27 nm	23.03 ± 2.00 MPa	103.75 ± 5.30%
PLCL/COL aligned fibers (perpendicular)	336.90 ± 107.27 nm	5.26 ± 0.31 MPa	116.02 ± 30.15%
PLCL/COL random fibers	361.15 ± 136.91 nm	15.73 ± 2.55 MPa	99.1 ± 14.57%
Single PLGA/SF yarn	206.17 ± 46.23 μm	15.57 ± 1.33 MPa	201.14 ± 17.16%

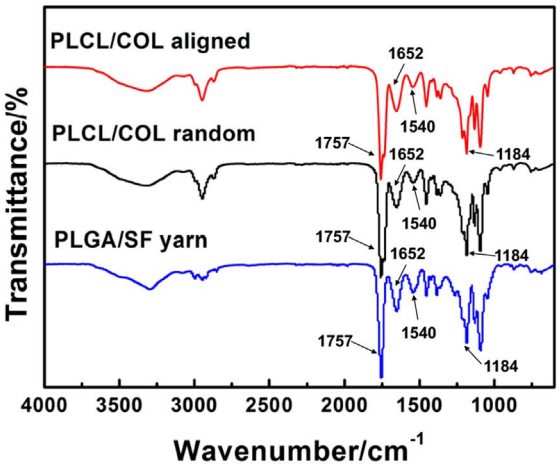

Fig. 3. FTIR analyses of PLCL/COL aligned and random fibers, and PLGA/SF yarns.

elongation of 103.75 ± 5.30% in the parallel direction, while the fibers possessed a stress at 5.26 ± 0.31 MPa and an elongation at 116.02 ± 30.15% in the perpendicular direction (Fig. 4A). The single PLGA/SF yarn in the middle layer showed a 15.57 ± 1.33 MPa and an elongation at 201.14 ± 17.16%, respectively (Fig. 4B). The PLCL/COL random fibers had a tensile stress of 15.73 ± 2.55 MPa and an elongation of 99.1 ± 14.57% (Fig. 4C). The tensile mechanical stress and elongation values are summarized in Table 1, and the results show that each layer of the scaffold can provide good mechanical support when stretched. Fig. 4D-F shows the tensile and compressive mechanical properties of the tri-layer tubular graft. The tubular graft presented the tensile force around 50 N and the strain around 100% along the axial direction (Fig. 4D). Fig. 4E and F shows that the graft had compressive and resilience properties in the radial direction, which could support 50% compressive strain even after 10 compressive cycles. The results demonstrate the suitable behaviour of the tri-layer graft in mechanical performance.

3.4. HUVECs proliferation on PLCL/COL fibers

Fig. 5A shows HUVECs proliferation on PLCL/COL random and aligned fibers after culturing for 6 days. At day 1, HUEVCs proliferation on TCP was significantly better ($P < 0.05$) than fibers. Subsequently, HUVECs proliferated on PLCL/COL fibers in an accelerated way and showed a significant difference ($P < 0.05$) from TCP at day 3. Finally, no significant difference was observed among the different groups at day 6. At each time point, there was no significant difference between PLCL/COL random and aligned fibers, indicating the slight effect of fiber alignment on HUVECs proliferation. The fluorescence images in Fig. 5A display HUVECs morphology on PLCL/COL fibers and TCP after culturing for 3 days. Fiber alignment presented a significant influence on cell morphology. HUVECs on PLCL/COL random fibers and TCP showed disordered shapes, and cells on PLCL random fibers had better interconnection than those on TCP. In comparison, HUVECs on PLCL/COL aligned fibers showed better orientation along the direction of fibers, and cells presented superior interaction as well. The orientated HUVECs in the inner surface will encourage the well growth of organized endothelium and regulate biological signaling events to improve lumen patency [31,47].

3.5. SMCs proliferation on PLGA/SF yarns

Fig. 5B presents SMCs proliferation on PLGA/SF fibers and yarns after culturing for 6 days. At every period, SMCs proliferation on PLGA/SF yarns had a significant difference ($P < 0.05$) from PLGA/SF fibers. Besides, SMCs growth on PLGA/SF yarns performed significantly better ($P < 0.05$) than TCP as well. This can be attributed to the fact that three-dimensional yarns provide more growth space and specific surface area for cell growth [40,48]. The fluorescence images in Fig. 5B show SMCs growth morphology on PLGA/SF fibers, PLGA/SF yarns and TCP after culturing for 3 days. Because of the random distribution of PLGA/SF fibers and non-structured surface of TCP, SMCs spread with disordered organization on these substrates. In comparison, SMCs spread along the direction of PLGA/SF yarns. The three-dimensional structure and oriented distribution of PLGA/SF yarns guided SMCs organization and proliferation, which would be responsible for the mechanical support and structure maintenance of the media wall for vascular graft [49–51].

3.6. Histological analysis after subcutaneous implantation

Fig. 6A–C demonstrates the gross morphology of the tri-layer tubular graft after subcutaneous implantation for 2, 6 and 10 weeks. The

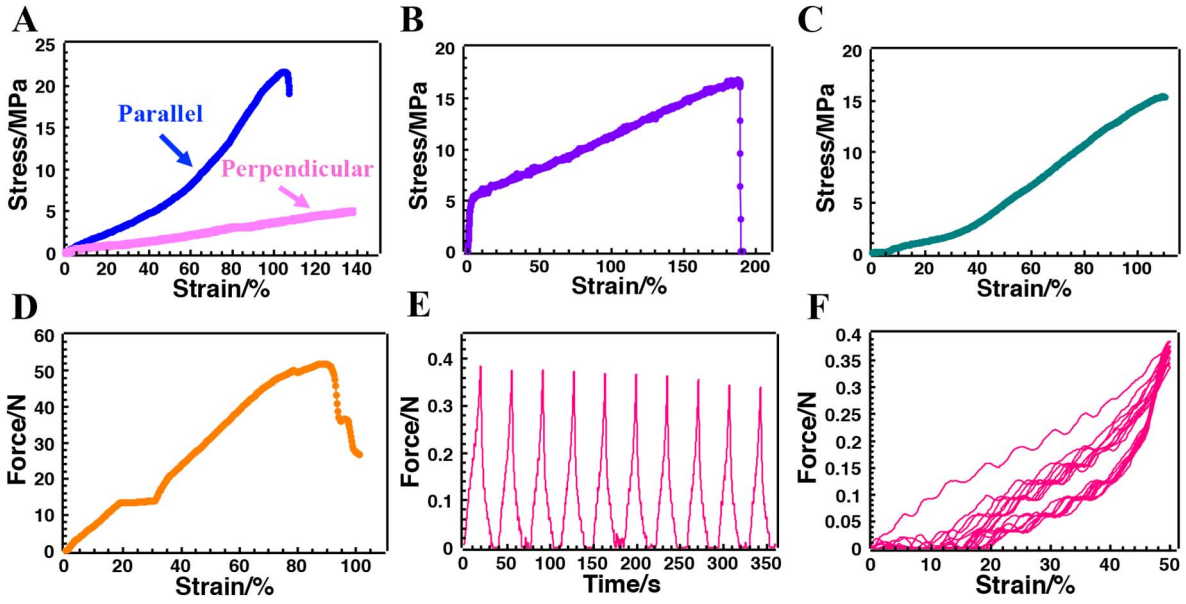

Fig. 4. Mechanical properties tests: the tensile strain-stress curves of (A) PLCL/COL aligned fibers, (B) PLGA/SF yarns, (C) PLCL/COL random fibers, and (D) the tri-layer tubular graft in the axial direction; the compressive (E) time-force curve and (F) strain-force curve of the tri-layer tubular graft in the radial direction.

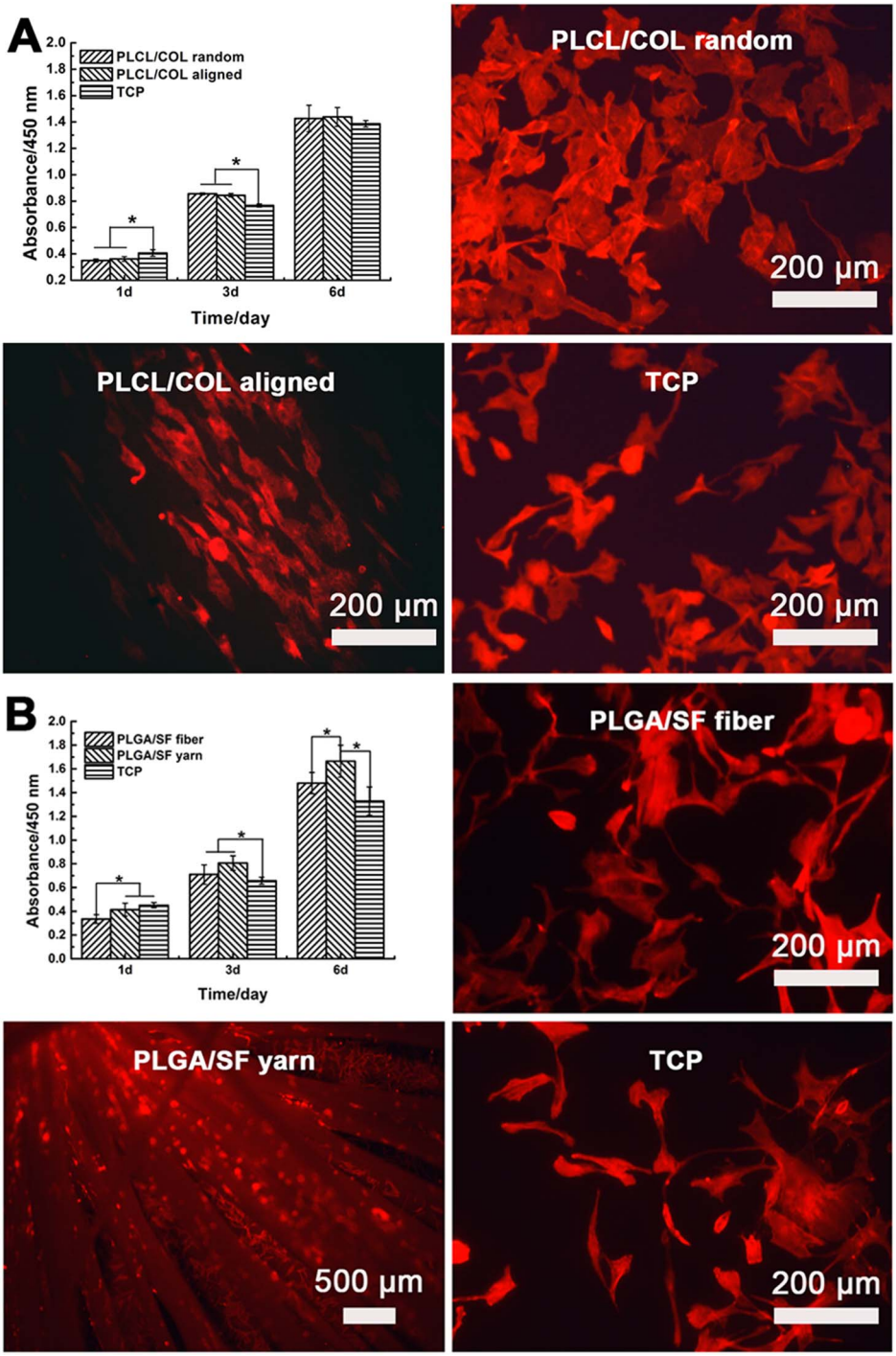

Fig. 5. (A) HUVECs growth on different samples: CCK-8 results of HUVECs proliferation on PLCL/COL aligned and random fibers after culturing for 1, 3 and 6 days; The fluorescence images showing HUVECs morphologies on PLCL/COL random fibers, PLCL/COL aligned fibers and TCP after incubating for 3 days; (B) SMCs growth on different samples: CCK-8 results of SMCs proliferation on PLGA/SF fibers and yarns after culturing for 1, 3 and 6 days; The fluorescence images showing SMCs morphologies on PLGA/SF fibers, PLGA/SF yarns and TCP after incubating for 3 days. * indicated the significant difference at $P < 0.05$ level.

Fig. 6. The general morphology of the transplanted grafts after subcutaneous embedding in mice for 2 weeks (A), 6 weeks (B) and 10 weeks (C).

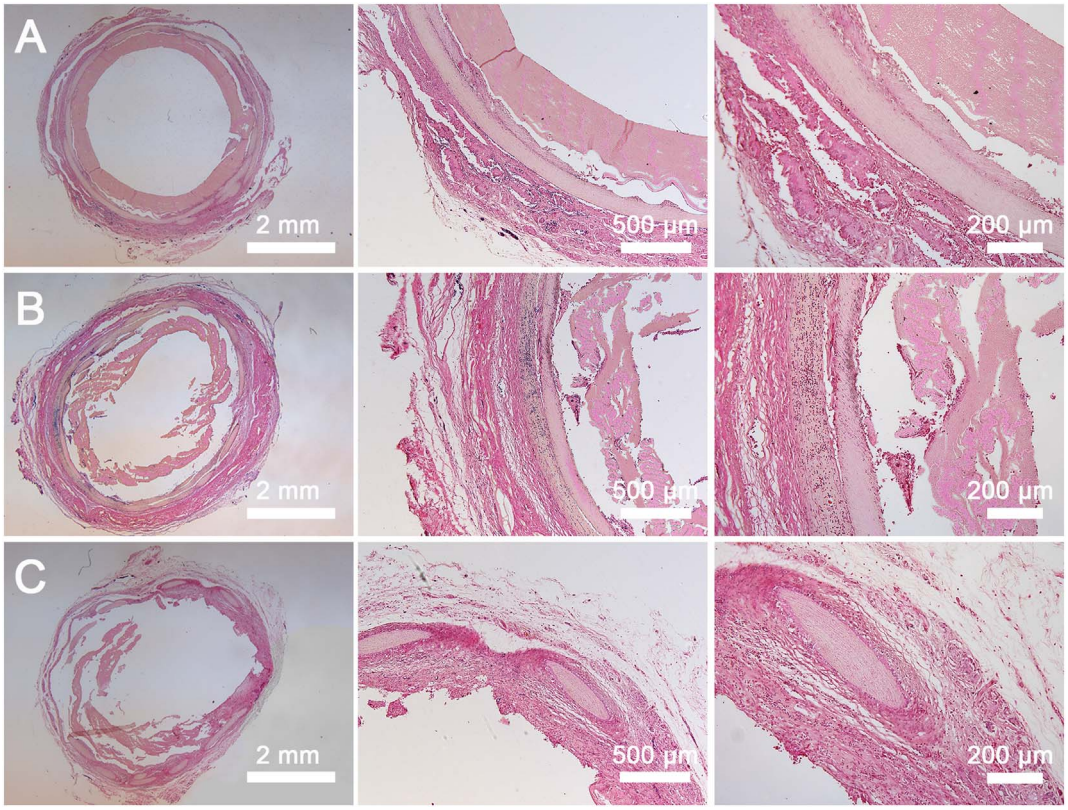

Fig. 7. H & E staining images of the transplanted grafts after subcutaneous embedding in mice for 2 weeks (A), 6 weeks (B) and 10 weeks (C).

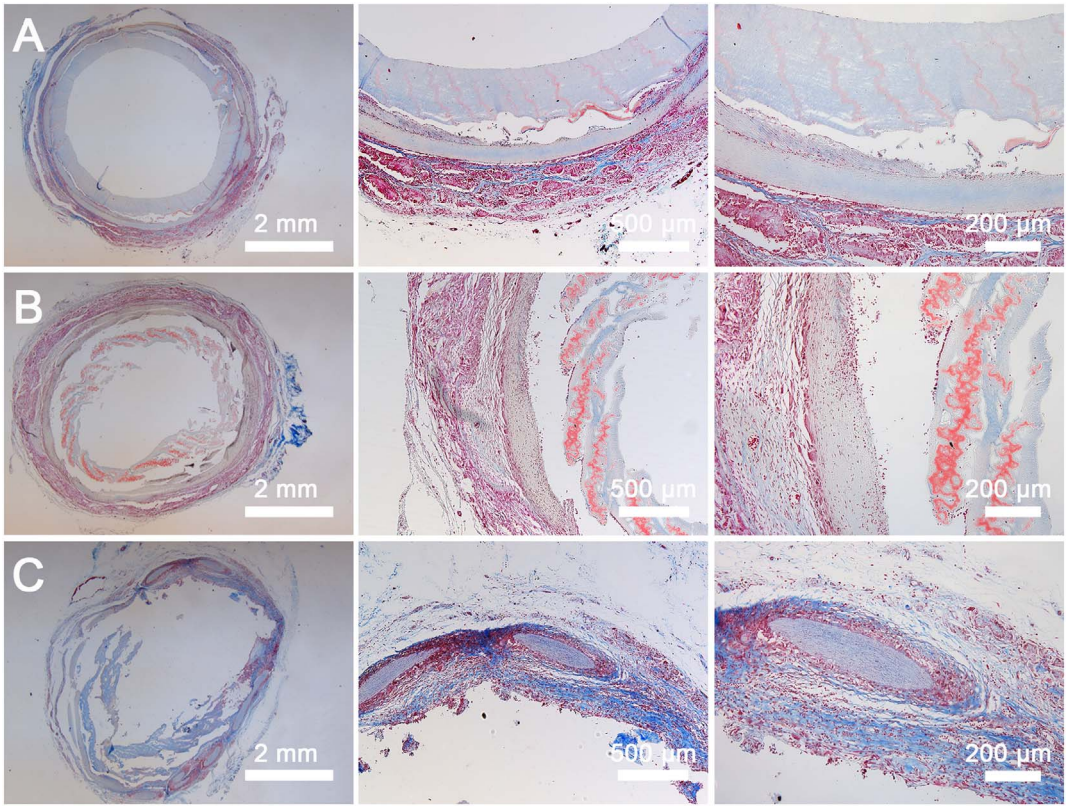

Fig. 8. Masson's trichrome staining images of the transplanted grafts after subcutaneous embedding in mice for 2 weeks (A), 6 weeks (B) and 10 weeks (C).

grafts were wrapped by the autologous tissues and kept the tubular structure during all implantation periods. Then, histological analysis of transverse sections at the middle sites were conducted by H & E staining (Fig. 7) and Masson's trichrome staining (Fig. 8). The typical H & E images showed cell infiltration and graft degradation after the grafts were subcutaneously implanted for 2, 6 and 10 weeks. At 2 weeks, the graft maintained the integral structure and cells proliferated on the outside surface of the graft (Fig. 7A). A layer of regenerated tissues was formed at the exterior of the graft. After subcutaneous embedding for 6 weeks, cells migrated and penetrated from the outside surface to the interior of the graft (Fig. 7B). It has been reported that cells can infiltrated into the interior of the electrospun scaffolds based on nanofiber yarns due to the porous structure [41,52–55]. Besides, the graft began to biodegrade, and some fragments of the graft layers were observed. The biodegradation of the tri-layer scaffold contributed to cell infiltration as well. After subcutaneous implantation for 10 weeks, the cells infiltrated into the entire graft and the graft was wrapped by the tissues surrounding the graft wall (Fig. 7C). Much more fragments of the graft layers were produced and the fragments were encapsulated by cells and fibrous tissues. The whole graft structure was well-kept due to the regenerated tissues. During the subcutaneous implantation periods, the regenerated tissues surrounding the graft distributed uniformly.

The images of Masson's trichrome staining indicated the production of collagen fibers secreted by the infiltrated cells (Fig. 8). As expected, collagen regeneration was increased with the time during the subcutaneous implantation periods. At the beginning 2 weeks, collagen formed on the outer layer surface of the graft (Fig. 8A). In comparison, abundant collagen components (blue fibers) were produced and infiltrated into the tri-layer graft after implanting for 10 weeks (Fig. 8C). The regenerated collagen fibers enclosed the graft fragments and maintained the integral graft structure. It indicated that the infiltrated cells preserved the functionality and the produced collagen fibers provided a biomimetic microenvironment for tissue regeneration [56]. The overall results demonstrated that the tri-layer tubular graft performed biodegradability, biocompatibility, collagen regeneration and cell infiltration capability during the subcutaneous implantation.

The tri-layer vascular scaffold is composed of PLCL/collagen fibers and PLGA/SF fiber yarns. The PLCL/collagen fibers in inner and outer layers are used for maintaining the tubular structure during *in vivo* implantation, while the porous PLGA/SF fiber yarns can be controllably biodegraded to support cells infiltration into the interior of the scaffold. Histological analyses in Fig. 7 and Fig. 8 demonstrate that the tri-layer scaffold biodegraded with tissue regeneration, and the layered structure was visible. After subcutaneous implantation for 10 weeks, the scaffold was loose and layered but still maintained the tubular structure. When applied this tri-layer scaffold to *in situ* implantation, the graft need to maintain the entire structure for a longer time to support vascular tissue regeneration. In this case, we can improve the structural stability and vary the biodegradability of the tri-layer graft by adjusting the layer thickness, gap distances between each layer, and the ratios of different polymers/proteins. Furthermore, we can modify the graft surface with heparin and vascular endothelial growth factor (VEGF) to avoid thrombus and accelerate endothelialization in the further study of *in situ* implantation. We expect the structural and functional simulation of the tri-layer graft will improve the outcome of vascular tissue regeneration and functionalization. Hence, this class of biomimetic tri-layer tubular graft will be worthy investigating the potential for vascular tissue regeneration and remolding in large animals.

4. Conclusion

The tri-layer tubular graft was designed and fabricated by a three-step electrospinning method for vascular tissue engineering. The tri-layer vascular graft consisted of axially aligned PLCL/COL fibers in the inner layer, circumferentially oriented PLGA/SF yarns in the middle layer, and random PLCL/COL fibers as the fixed layer outside. The fibers and yarns in each layer as well as the entire tubular graft had good mechanical properties to support tensile and compressive strength. *In vitro* studies demonstrated that the aligned PLCL/COL fibers and PLGA/SF yarns separately promoted endothelia and smooth muscle cells proliferation and organization along the fiber direction. The histological results after subcutaneous implantation for 10 weeks *in vivo* further demonstrated that the tri-layer tubular graft possessed biodegradability and promoted cell infiltration from the microenvironment into the interior of the graft. For further improvement, we can vary the graft biodegradability by adjusting the layer thickness, gap distances between each layer, and the ratios of different polymers/proteins. Moreover, we can modify the graft surface with biological cues to avoid thrombus and accelerate endothelialization when using the graft for *in situ* implantation. We expect the structural and functional simulation of the tri-layer graft will improve the outcome of vascular tissue regeneration and functionalization. Hence, the biomimetic tri-layer vascular graft provided an encouraging substitute for vascular tissue engineering, which would be worthy further considering for vascular tissue regeneration in large animals.

Acknowledgment

This research was supported by the National Major Research Program of China (2016YFC1100202), National Natural Science Foundation of China (31470941, 81671833), Science and Technology Commission of Shanghai Municipality (15JC1490100, 15441905100), Fundamental Research Funds for the Central Universities (CUSF-DH-D-2017047), light of textile project (J201404), Pudong New Area Science and Technology Development Fund Minsheng Scientific Research (Medical and Health) Project (PKJ2016-Y33), Collaborative Innovation Center for Translational Medicine (TM201504) and Ai You Foundation (2017SCMC-AY002). The authors would like to extend their sincere appreciation to the Deanship of Scientific Research at King Saud University for its funding through the research group project (No. RGP-201).

References

[1] S. Pashneh-Tala, S. MacNeil, F. Claeyssens, The tissue-engineered vascular graft-past, present, and future, Tissue Eng. B Rev. 22 (2015) 68–100.
[2] W.A. Zoghbi, T. Duncan, E. Antman, M. Barbosa, B. Champagne, D. Chen, H. Gamra, J.G. Harold, S. Josephson, M. Komajda, Sustainable development goals and the future of cardiovascular health: a statement from the Global Cardiovascular Disease Taskforce, J. Am. Heart Assoc. 3 (2014) e000504.
[3] X. Ren, Y. Feng, J. Guo, H. Wang, Q. Li, J. Yang, X. Hao, J. Lv, N. Ma, W. Li, Surface modification and endothelialization of biomaterials as potential scaffolds for vascular tissue engineering applications, Chem. Soc. Rev. 44 (2015) 5680–5742.
[4] K.A. Rocco, M.W. Maxfield, C.A. Best, E.W. Dean, C.K. Breuer, In vivo applications of electrospun tissue-engineered vascular grafts: a review, Tissue Eng. B Rev. 20 (2014) 628–640.
[5] J. Hu, D. Kai, H. Ye, L. Tian, X. Ding, S. Ramakrishna, X.J. Loh, Electrospinning of poly(glycerol sebacate)-based nanofibers for nerve tissue engineering, Mater Sci Eng C Mater Biol Appl 70 (2017) 1089–1094.
[6] D. Kai, S. Jiang, Z.W. Low, X.J. Loh, Engineering highly stretchable lignin-based electrospun nanofibers for potential biomedical applications, J. Mater. Chem. B 3 (2015) 6194–6204.
[7] D. Kai, S.S. Liow, X.J. Loh, Biodegradable polymers for electrospinning: towards biomedical applications, Mater Sci Eng C Mater Biol Appl 45 (2014) 659–670.
[8] D. Kai, M.P. Prabhakaran, B.Q. Chan, S.S. Liow, S. Ramakrishna, F. Xu, X.J. Loh, Elastic poly(epsilon-caprolactone)-polydimethylsiloxane copolymer fibers with shape memory effect for bone tissue engineering, Biomed. Mater. 11 (2016) 015007.
[9] D. Kai, W. Ren, L. Tian, P.L. Chee, Y. Liu, S. Ramakrishna, X.J. Loh, Engineering poly(lactide)–lignin nanofibers with antioxidant activity for biomedical application, ACS Sustain. Chem. Eng. 4 (2016) 5268–5276.
[10] D. Kai, M.J. Tan, M.P. Prabhakaran, B.Q. Chan, S.S. Liow, S. Ramakrishna, X.J. Loh, Biocompatible electrically conductive nanofibers from inorganic-organic shape memory polymers, Colloids Surf. B: Biointerfaces 148 (2016) 557–565.
[11] R. Lakshminarayanan, R. Sridhar, X.J. Loh, M. Nandhakumar, V.A. Barathi, M. Kalaipriya, J.L. Kwan, S.P. Liu, R.W. Beuerman, S. Ramakrishna, Interaction of gelatin with polyenes modulates antifungal activity and biocompatibility of electrospun fiber mats, Int. J. Nanomedicine 9 (2014) 2439–2458.
[12] X.J. Loh, P. Peh, S. Liao, C. Sng, J. Li, Controlled drug release from biodegradable thermoresponsive physical hydrogel nanofibers, J. Control. Release 143 (2010)

175–182.
[13] M. Zhu, K. Wang, J. Mei, C. Li, J. Zhang, W. Zheng, D. An, N. Xiao, Q. Zhao, D. Kong, Fabrication of highly interconnected porous silk fibroin scaffolds for potential use as vascular grafts, Acta Biomater. 10 (2014).
[14] S. Liu, C. Dong, G. Lu, Q. Lu, Z. Li, D.L. Kaplan, H. Zhu, Bilayered vascular grafts based on silk proteins, Acta Biomater. 9 (2013) 8991–9003.
[15] A. Hasan, A. Memic, N. Annabi, M. Hossain, A. Paul, M.R. Dokmeci, F. Dehghani, A. Khademhosseini, Electrospun scaffolds for tissue engineering of vascular grafts, Acta Biomater. 10 (2014) 11–25.
[16] V. Catto, S. Farè, G. Freddi, M.C. Tanzi, Vascular tissue engineering: recent advances in small diameter blood vessel regeneration, ISRN Vascular Medicine 2014 (2014).
[17] V. Catto, S. Farè, I. Cattaneo, M. Figliuzzi, A. Alessandrino, G. Freddi, A. Remuzzi, M.C. Tanzi, Small diameter electrospun silk fibroin vascular grafts: mechanical properties, in vitro biodegradability, and in vivo biocompatibility, Mater Sci Eng C Mater Biol Appl 54 (2015) 101–111.
[18] T. Wu, C. Huang, D. Li, A. Yin, W. Liu, J. Wang, J. Chen, H. Ei-Hamshary, S.S. Al-Deyab, X. Mo, A multi-layered vascular scaffold with symmetrical structure by bi-directional gradient electrospinning, Colloids Surf. B: Biointerfaces 133 (2015) 179–188.
[19] C.P. Barnes, S.A. Sell, E.D. Boland, D.G. Simpson, G.L. Bowlin, Nanofiber technology: designing the next generation of tissue engineering scaffolds, Adv. Drug Deliv. Rev. 59 (2007) 1413–1433.
[20] J. Hu, X. Sun, H. Ma, C. Xie, Y.E. Chen, P.X. Ma, Porous nanofibrous PLLA scaffolds for vascular tissue engineering, Biomaterials 31 (2010) 7971–7977.
[21] Y. Liu, C. Jiang, S. Li, Q. Hu, Composite vascular scaffold combining electrospun fibers and physically-crosslinked hydrogel with copper wire-induced grooves structure, J. Mech. Behav. Biomed. Mater. 61 (2016) 12–25.
[22] C.M. O'Brien, B. Holmes, S. Faucett, L.G. Zhang, Three-dimensional printing of nanomaterial scaffolds for complex tissue regeneration, Tissue Eng. B Rev. 21 (2014) 103–114.
[23] H. Zhang, X. Jia, F. Han, J. Zhao, Y. Zhao, Y. Fan, X. Yuan, Dual-delivery of VEGF and PDGF by double-layered electrospun membranes for blood vessel regeneration, Biomaterials 34 (2013) 2202–2212.
[24] F. Han, X. Jia, D. Dai, X. Yang, J. Zhao, Y. Zhao, Y. Fan, X. Yuan, Performance of a multilayered small-diameter vascular scaffold dual-loaded with VEGF and PDGF, Biomaterials 34 (2013) 7302–7313.
[25] S. de Valence, J.C. Tille, J.P. Giliberto, W. Mrowczynski, R. Gurny, B.H. Walpoth, M. Moller, Advantages of bilayered vascular grafts for surgical applicability and tissue regeneration, Acta Biomater. 8 (2012) 3914–3920.
[26] Z. Wang, Y. Cui, J. Wang, X. Yang, Y. Wu, K. Wang, X. Gao, D. Li, Y. Li, X.L. Zheng, Y. Zhu, D. Kong, Q. Zhao, The effect of thick fibers and large pores of electrospun poly(epsilon-caprolactone) vascular grafts on macrophage polarization and arterial regeneration, Biomaterials 35 (2014) 5700–5710.
[27] M.J. McClure, S.A. Sell, D.G. Simpson, B.H. Walpoth, G.L. Bowlin, A three-layered electrospun matrix to mimic native arterial architecture using polycaprolactone, elastin, and collagen: a preliminary study, Acta Biomater. 6 (2010) 2422–2433.
[28] M.J. McClure, D.G. Simpson, G.L. Bowlin, Tri-layered vascular grafts composed of polycaprolactone, elastin, collagen, and silk: optimization of graft properties, J. Mech. Behav. Biomed. Mater. 10 (2012) 48–61.
[29] S.G. Wise, M.J. Byrom, A. Waterhouse, P.G. Bannon, A.S. Weiss, M.K. Ng, A multilayered synthetic human elastin/polycaprolactone hybrid vascular graft with tailored mechanical properties, Acta Biomater. 7 (2011) 295–303.
[30] Y.M. Ju, J.S. Choi, A. Atala, J.J. Yoo, S.J. Lee, Bilayered scaffold for engineering cellularized blood vessels, Biomaterials 31 (2010) 4313–4321.
[31] Y.M. Shin, H.J. Shin, Y. Heo, I. Jun, Y.-W. Chung, K. Kim, Y.M. Lim, H. Jeon, H. Shin, Engineering an aligned endothelial monolayer on a topologically modified nanofibrous platform with a micropatterned structure produced by femtosecond laser ablation, J. Mater. Chem. B 5 (2017) 318–328.
[32] Y.-S.J. Li, J.H. Haga, S. Chien, Molecular basis of the effects of shear stress on vascular endothelial cells, J. Biomech. 38 (2005) 1949–1971.
[33] C. Galbraith, R. Skalak, S. Chien, Shear stress induces spatial reorganization of the endothelial cell cytoskeleton, Cell Motil. Cytoskeleton 40 (1998) 317–330.
[34] S. Noria, D.B. Cowan, A.I. Gotlieb, B.L. Langille, Transient and steady-state effects of shear stress on endothelial cell adherens junctions, Circ. Res. 85 (1999) 504–514.
[35] G.K. Owens, Regulation of differentiation of vascular smooth muscle cells, Physiol. Rev. 75 (1995) 487–517.
[36] A.J. Bank, H. Wang, J.E. Holte, K. Mullen, R. Shammas, S.H. Kubo, Contribution of collagen, elastin, and smooth muscle to in vivo human brachial artery wall stress and elastic modulus, Circulation 94 (1996) 3263–3270.
[37] S.P. Hoerstrup, G. Zünd, R. Sodian, A.M. Schnell, J. Grünenfelder, M.I. Turina, Tissue engineering of small caliber vascular grafts, Eur. J. Cardiothorac. Surg. 20 (2001) 164–169.
[38] J.D. Kakisis, C.D. Liapis, C. Breuer, B.E. Sumpio, Artificial blood vessel: the Holy Grail of peripheral vascular surgery, J. Vasc. Surg. 41 (2005) 349–354.
[39] K. Zhang, H. Wang, C. Huang, Y. Su, X. Mo, Y. Ikada, Fabrication of silk fibroin blended P(LLA-CL) nanofibrous scaffolds for tissue engineering, J. Biomed. Mater. Res. A 93 (2010) 984–993.
[40] T. Wu, H. Zheng, J. Chen, Y. Wang, B. Sun, Y. Morsi, H. El-Hamshary, S.S. Al-Deyab, C. Chen, X. Mo, Application of a bilayer tubular scaffold based on electrospun poly (l-lactide-co-caprolactone)/collagen fibers and yarns for tracheal tissue engineering, J. Mater. Chem. B 5 (2017) 139–150.
[41] Y. Xu, S. Dong, Q. Zhou, X. Mo, L. Song, T. Hou, J. Wu, S. Li, Y. Li, P. Li, Y. Gan, J. Xu, The effect of mechanical stimulation on the maturation of TDSCs-poly(L-lactide-co-e-caprolactone)/collagen scaffold constructs for tendon tissue engineering, Biomaterials 35 (2014) 2760–2772.
[42] T. Wu, B. Jiang, Y. Wang, A. Yin, C. Huang, S. Wang, X. Mo, Electrospun poly(l-lactide-co-caprolactone)–collagen–chitosan vascular graft in a canine femoral artery model, J. Mater. Chem. B 3 (2015) 5760–5768.
[43] A.F. Sulong, N.H. Hassan, N.M. Hwei, Y. Lokanathan, A.S. Naicker, S. Abdullah, M.R. Yusof, O. Htwe, R. Idrus, N. Haflah, Collagen-coated polylactic-glycolic acid (PLGA) seeded with neural-differentiated human mesenchymal stem cells as a potential nerve conduit, Adv. Clin. Exp. Med. 23 (2014) 353–362.
[44] Y. Xu, J. Wu, H. Wang, H. Li, N. Di, L. Song, S. Li, D. Li, Y. Xiang, W. Liu, X. Mo, Q. Zhou, Fabrication of electrospun poly(L-lactide-co-epsilon-caprolactone)/collagen nanoyarn network as a novel, three-dimensional, macroporous, aligned scaffold for tendon tissue engineering, Tissue Eng. Part C Methods 19 (2013) 925–936.
[45] B. Sun, T. Wu, J. Wang, D. Li, J. Wang, Q. Gao, M.A. Bhutto, H. El-Hamshary, S.S. Al-Deyab, X. Mo, Polypyrrole-coated poly(l-lactic acid-co-ε-caprolactone)/silk fibroin nanofibrous membranes promoting neural cell proliferation and differentiation with electrical stimulation, J. Mater. Chem. B 4 (2016) 6670–6679.
[46] O. Evrova, V. Hosseini, V. Milleret, G. Palazzolo, M. Zenobi-Wong, T. Sulser, J. Buschmann, D. Eberli, Hybrid randomly electrospun PLGA:PEO fibrous scaffolds enhancing myoblast differentiation and alignment, ACS Appl. Mater. Interfaces 8 (2016) 31574–31586.
[47] Y.S. Li, J.H. Haga, S. Chien, Molecular basis of the effects of shear stress on vascular endothelial cells, J. Biomech. 38 (2005) 1949–1971.
[48] J. Wu, C. Huang, W. Liu, A. Yin, W. Chen, C. He, H. Wang, S. Liu, C. Fan, G.L. Bowlin, Cell infiltration and vascularization in porous nanoyarn scaffolds prepared by dynamic liquid electrospinning, J. Biomed. Nanotechnol. 10 (2014) 603–614.
[49] E. Vatankhah, M.P. Prabhakaran, D. Semnani, S. Razavi, M. Zamani, S. Ramakrishna, Phenotypic modulation of smooth muscle cells by chemical and mechanical cues of electrospun tecophilic/gelatin nanofibers, ACS Appl. Mater. Interfaces 6 (2014) 4089–4101.
[50] Y. Wang, H. Shi, J. Qiao, Y. Tian, M. Wu, W. Zhang, Y. Lin, Z. Niu, Y. Huang, Electrospun tubular scaffold with circumferentially aligned nanofibers for regulating smooth muscle cell growth, ACS Appl. Mater. Interfaces 6 (2014) 2958–2962.
[51] J.M. Thayer, K. Meyers, C.M. Giachelli, S.M. Schwartz, Formation of the arterial media during vascular development, Cell. Mol. Biol. Res. 41 (1995) 251–262.
[52] J. Wu, S. Liu, L. He, H. Wang, C. He, C. Fan, X. Mo, Electrospun nanoyarn scaffold and its application in tissue engineering, Mater. Lett. 89 (2012) 146–149.
[53] J. Wu, Y. Hong, Enhancing cell infiltration of electrospun fibrous scaffolds in tissue regeneration, Bioactive Materials 1 (2016) 56–64.
[54] X. Zheng, W. Wang, S. Liu, J. Wu, F. Li, L. Cao, X.D. Liu, X. Mo, C. Fan, Enhancement of chondrogenic differentiation of rabbit mesenchymal stem cells by oriented nanofiber yarn-collagen type I/hyaluronate hybrid, Mater Sci Eng C Mater Biol Appl 58 (2016) 1071–1076.
[55] S. Liu, J. Wu, X. Liu, D. Chen, G.L. Bowlin, L. Cao, J. Lu, F. Li, X. Mo, C. Fan, Osteochondral regeneration using an oriented nanofiber yarn-collagen type I/hyaluronate hybrid/TCP biphasic scaffold, J. Biomed. Mater. Res. A 103 (2015) 581–592.
[56] J. Zhang, J. Du, D. Xia, J. Liu, T. Wu, J. Shi, W. Song, D. Jin, X. Mo, M. Yin, Preliminary study of a novel nanofiber-based valve integrated tubular graft as an alternative for a pulmonary valved artery, RSC Adv. 6 (2016) 84837–84846.